

Endosomal maturation leads to nucleocapsid conformation change in seasonal coronaviruses

Miki Umeda¹, Koji Yoshimura¹, Yoshitaka Sato¹, Yasuyuki Miyake^{1,2}
and Hiroshi Kimura¹

¹*Department of Virology, Nagoya University Graduate School of Medicine, Nagoya, Japan*
²*Nagoya University Institute for Advanced Research (IAR), Nagoya, Japan*

ABSTRACT

As seen in the coronavirus pandemic, the social impact of the spread of emerging and re-emerging viral infections is significant. Whilst seasonal human coronaviruses with common cold symptoms have long been identified, there are only few studies on cellular entry pathway into host cells. Human coronavirus (HCoV)-229E, which has a positive single-stranded RNA genome, binds to the host cell surface receptor Aminopeptidase N and is taken up into the cell by endocytosis. The viral genome is then released from the endosome into the cytoplasm via uncoating step, the molecular mechanism of which remains unclear. In the uncoating of influenza A viruses, it is known that after membrane fusion in matured endosomes, unanchored ubiquitin chains present in the viral particle are exposed to the cytoplasmic side, which recruits the host factor histone deacetylase 6 (HDAC6) and promotes M1 uncoating. In this study, purified virus particles were used to investigate the involvement of ubiquitin in the uncoating of coronaviruses, and their properties were determined. The results show that there are few unanchored ubiquitin chains in coronavirus particles, suggesting that they use ubiquitin-independent uncoating different from influenza A virus. More interestingly, acidification within the endosome leads to nucleocapsid condensate formation *in vitro*. From these results, we would like to propose a new model that coronaviruses with long single-stranded RNA genomes efficiently uncoat their genomes by forming condensates during uncoating, thereby evading the innate immune response from the host. Understanding these molecular mechanisms is expected to lead to drug development.

Keywords: HCoV-229E, ubiquitin, nucleoprotein, viral entry, uncoating

Abbreviations:

HCoV: human coronavirus

vRNP: viral ribonucleoprotein

IAV: influenza A virus

VCP: valosin-containing protein

This is an Open Access article distributed under the Creative Commons Attribution-NonCommercial-NoDerivatives 4.0 International License. To view the details of this license, please visit (<http://creativecommons.org/licenses/by-nc-nd/4.0/>).

Received: May 26, 2025; Accepted: August 8, 2025

Corresponding Author: Yasuyuki Miyake, PhD

Department of Virology, Nagoya University Graduate School of Medicine,

65 Tsurumai-cho, Showa-ku, Nagoya 466-8550, Japan

Tel: +81-52-744-2451, E-mail: yasumiya@med.nagoya-u.ac.jp

INTRODUCTION

SARS-CoV-2, which has caused a global pandemic since the end of 2019, has had an unprecedented socio-economic impact. Much remains unknown about the mechanisms of replication in host cells of not only SARS-CoV-2 but also seasonal coronaviruses causing common cold symptoms. Coronaviruses have a positive single-stranded RNA genome of approximately 30 kb and the old known seasonal strains infecting humans are human coronavirus (HCoV)-OC43, HCoV-229E, HCoV-NL63 and HCoV-HKU1, with SARS-CoV, MERS-CoV and SARS-CoV-2 which have been classified as causing severe acute respiratory syndromes.¹ Viruses can infect and amplify by hijacking various biological functions of the host cells.

It has long been well known that HCoV-229E enters cells by endocytosis.² HCoV-229E attaches to human Aminopeptidase N present on the host cell surface as receptors and penetrates the endosomes.³ The spike protein is cleaved by cathepsin L present in intracellular endosomes, causing membrane fusion. Acidification within endosomes is thought to be important for fusion with the endosomal membrane through conformational changes of spike proteins on the viral membrane surface, but the other functional significance remains unclear. Alternative pathway is membrane fusion at the cell surface following cleavage by transmembrane protease serine 2 (TMPRSS2), which has been reported to be the predominant pathway used in clinical strains.⁴

Influenza A virus (IAV), which like coronaviruses is well-known to cause respiratory infections, has an eight-segmented genome and penetrates the cells by endocytosis after binding to the host cell surface. When the endosome matures, haemagglutinin (HA) on the viral membrane undergoes a conformational change due to prevailing lower pH condition of the endosomal microenvironment, resulting in a fusion of the virus-endosome membranes and uncoating of the viral ribonucleoprotein complex (vRNPs) from the endosome.^{5,6} As IAV has unanchored ubiquitin chains in the viral particles, vRNPs are released into the cytoplasm after M1 shell disassembly by the ubiquitin-binding and Dynein-binding activities of the host deacetylase HDAC6.^{7,8} Then, vRNPs are dissociated into respective segments by the host nuclear import factor TNPO1.^{7,9} Dissociation into each segment allows individual vRNP to pass through the nuclear pore complex and to be transcribed and replicated in the nucleus.¹⁰

Recent analysis of SARS-CoV-2 has suggested that genome packaging occurs through phase separation of viral genomic RNA and nucleoproteins.¹¹ It has also been reported that phosphorylation of nucleoproteins promotes the formation of liquid-liquid phase separation.¹² However, very little is known about the process of coronavirus uncoating from endosomes. In this study, we propose a novel mechanism by which seasonal coronaviruses are incorporated into endosomes and cause conformational changes in the viral genome by acidification within mature endosomes, leading to escape from the host innate immune response and efficient uncoating of the viral genome from endosomes to the cytosol.

MATERIALS AND METHODS

Cell line, viruses and chemicals

Human hepatoma Huh7 cells (RCB 1942; RIKEN BRC Cell Bank) were kindly provided from Dr Takayuki Murata and cultured in Dulbecco modified Eagle medium (DMEM; Nacalai Tesque) supplemented with 10% fetal bovine serum (FBS), penicillin and streptomycin (GIBCO), GlutaMAX (GIBCO), non-essential amino acid (SIGMA) at 37 °C with 5% CO₂. HCoV-229E or HCoV-OC43 were purchased from ATCC and amplified by Huh7 cells. Bafilomycin A1 was purchased from Cayman Chemical. Valosin-containing protein (VCP) inhibitor NMS-873 was

purchased from Selleck. All the buffers were passed through 0.22 μm filtration device (Merck). Cytoskeleton (CSK) buffer contains 10 mM PIPES pH6.8, 300 mM Sucrose, 150 mM NaCl, 3 mM MgCl_2 , 1 mM EGTA.

Anti-nucleoprotein (N) antibody production

The anti-peptide antibodies were made on order from Cosmo Bio CO, LTD. Briefly, HCoV-229E derived peptide (C-SRSQRSRSQRGRGES) was synthesized and immunized into rabbit. IgG was affinity purified from obtained antisera.

Antibodies

The antibodies used in this study were: anti- β -actin (mouse monoclonal), anti-nucleoprotein (anti-peptide antibody produced in this study; see antibody production), anti-Rab5A (#R28720, BD Transduction Laboratories), anti-EEA1 (#610456, BD Transduction Laboratories), anti-dsRNA (K1: 28764S, Cell Signaling Technologies), anti-ubiquitin (FK2: D058-3, MBL; P4D1: ab139101, Abcam; A-5: sc-166553, Santa Cruz Biotechnology), anti-diglycyl lysine (GX41: MABS27, Merck), anti-mouse IgG HRP-conjugated (Cell Signaling Technology), anti-rabbit IgG HRP-conjugated (Cell Signaling Technology), anti-mouse IgG Alexa488-conjugated (Thermo Fisher), anti-rabbit IgG Alexa594-conjugated (Thermo Fisher).

Coronavirus purification

HCoV-229E and HCoV-OC43 were harvested from Huh7 cell culture supernatant, and infected to Huh7 cell line in T125 flask. Infected Huh7 cells were left in 35 °C for more than 1 week until all cells died. The cells were then frozen at -80 °C once to destroy them. After freezing and thawing, the supernatant was collected and centrifuged at 15,000 rpm for 20 minutes at 4 °C to remove cellular debris. The supernatant was centrifuged again at 20,000 rpm for 1 hour at 4 °C to precipitate the virus particles. The supernatant was removed and the precipitated virus was resuspended in 4-(2-hydroxyethyl)-1-piperazinyl ethanesulfonic acid (HEPES) buffer (pH 6.5), after which the virus fraction was fractionated by 10–50% sucrose density gradient ultracentrifugation at 100,000 $\times g$, 4 °C for 90 minutes with Optima XPN-80 Sw41Ti (Beckman). All fractions obtained were confirmed by Sodium dodecyl sulfate polyacrylamide gel electrophoresis (SDS-PAGE) followed by instantBlue staining (Abcam), the viral fractions were collected and concentrated by AmiconUltra 100 kDa MWCO concentration device (Merck) to obtain the final purified virus.

Plaque assay (tissue culture infectious dose 50)

The viral titer was determined by plaque assay. Huh7 cells were spread in 96 well flat bottom plate. The next day, dilution range of purified viruses was prepared and infected at 35 °C in 5% CO_2 . At seven days post-infection, cells were fixed with 4% paraformaldehyde and stained with 0.05% crystal violet. Tissue culture infectious dose 50 (TCID₅₀) was calculated from the stained plates.

Quantitative real time-polymerase chain reaction

10^5 Huh7 cells per well were seeded onto 24 well plate (FALCON) and cultured overnight at 37 °C in 5% CO_2 . The next day, the cells were treated with Bafilomycin A1 for 4 hours, then infected with virus to multiplicity of infection (MOI)=1. Cells were harvested 24 hours post infection, and stored in -80 °C. Total RNA was purified using the RNeasy Mini Kit (QIAGEN) and reverse-transcribed to complementary DNA (cDNA) using FastGene Scriptase II cDNA 5x ReadyMix (NIPPON Genetics). Viral cDNA levels were measured and normalized

by glyceraldehyde-3-phosphate dehydrogenase (*GAPDH*) using the 7500 Fast DX Real Time-Polymerase Chain Reaction (RT-PCR) system (Applied Biosystems) and the following primers: For HCoV-229E, 5'-CAT ACT ATC AAC CCA TTC AAC AAG-3' and 5'-CAC GGC AAC TGT CAT GTA TT-3'; for HCoV-OC43, 5'-CGA TGA GGC TAT TCC GAC TAG GT-3' and 5'-CCT TCC TGA GCC TTC AAT ATA GTA ACC-3'; for *GAPDH*, 5'-TGC ACC ACC AAC TGC TAG C-3' and 5'-GGC ATG GAC TGT GGT CAT GAG-3'. Triplicate quantification data were represented by GraphPad Prism.

Transmission electron microscopy

STEM Cu100P elastic carbon grid (Oken) was hydrophilised with ion bombarder (PIB-10). Purified virus samples were adsorbed on the grid for 1 minute, followed by negative staining treatment with 2% uranyl acetate solution for 1 minute. The sample was observed with a transmission electron microscope (JEM-1400PLUS, JEOL).

SDS-PAGE and Western blotting

Purified virus samples were dissolved in 4x sample buffer (250 mM Tris-HCl, pH 6.8, 8% SDS, 40% glycerol, 20% 2-mercaptoethanol, 0.02% bromophenol blue) (BIO-RAD), heat treated at 95 °C, 5 minutes, and then quickly loaded onto 9% or 15% SDS-PAGE. After SDS-PAGE, transfer onto PVDF membranes (Merck), blocking with 5% skim milk (Wako Fujifilm), followed by primary antibody reaction. Primary antibodies were diluted to 1:1,000 and secondary antibodies to 1:3,000, and the primary antibodies were reacted at 4 °C overnight and secondary antibodies at room temperature for 1 hour. After the antibody reaction, signals were detected by Luminata Forte Western HRP Substrate (Millipore), and images were acquired on LuminoGraph II EM (ATTO).

Immunofluorescent staining

10⁴ Huh7 cells per well were seeded onto a cell culture microplate 96 well F-bottom (655090, Greiner) and cultured overnight. The next day, the cells were infected with virus to MOI=5 or 10. Half an hour or two hours post infection, cells were fixed with 4% paraformaldehyde, permeabilised with CSK buffer containing 0.5% Triton and blocked with 3% BSA/PBS. 1:500 diluted primary antibody reactions were performed overnight at 4 °C, followed by washing with PBS and secondary antibody reactions for 1 hour at room temperature. After PBS washing, cells were counterstained with 4'-6-diamidino-2-phenylindole (DAPI), and images acquired with CQ1 (Yokogawa), BZ-X800 (Keyence) or Axio Observer (Zeiss).

In vitro uncoating assay

Viral genome complex vRNPs were purified according to the method of Stauffer et al.^{13,14} Briefly, a Beckman Ultra-Clear tube (Beckman) was used, 25% glycerol cell lysis buffer (30 mM MES pH5.4, 150 mM NaCl, 25% (v/v) glycerol, 1% NP-40, 1x complete protease inhibitor) was prepared in the lower layer and 15% glycerol buffer (30 mM MES pH5.4, 150 mM NaCl, 15% (v/v) glycerol) in the upper layer, and the virus solution was added. Ultracentrifugation was performed at 55,000 x g, 12 °C for 150 minutes with Optima XPN-80 Sw41Ti (Beckman). After centrifugation, the supernatant was removed and the precipitate was dissolved in an appropriate volume of 1x MNT buffer (20 mM MES pH7.4, 30 mM Tris-HCl pH7.4, 100 mM NaCl). Purified vRNP samples were checked by transmission electron microscopy (TEM) imaging.

Mass spectrometry

The protein samples were digested by Trypsin Gold (Promega) or Asp-N (Promega) for 16 hours at 37 °C after reduction and alkylation followed by In-gel digestion kit (Pierce). The

peptides were analyzed by LC–MS using a Q Exactive mass spectrometer (Thermo Fisher Scientific) coupled to an UltiMate3000 RSLC nano LC system (Dionex) using a nano HPLC capillary column, 150 mm 75 µm i.d (Nikkyo Technos) via a nano electrospray ion source. Reversed-phase chromatography was performed with a linear gradient (0 minute, 5% B; 45 minutes, 100% B) of solvent A (2% acetonitrile with 0.1% formic acid) and solvent B (95% acetonitrile with 0.1% formic acid) at an estimated flow rate of 300 nL/min. A precursor ion scan was carried out using a 400–1600 mass to charge ratio (m/z) prior to MS2 analysis. MS2 scan was obtained for the 20 most intense peaks of each MS1 scan.

Data analysis

The raw data was processed using either Proteome Discoverer 1.4 (Thermo Fisher Scientific) in conjunction with MASCOT search engine, version 2.7.0 (Matrix Science) for protein identification. Peptides and proteins were identified against virus protein database in UniProt (release 2022.01), with a precursor mass tolerance of 10 ppm, a fragment ion mass tolerance of 0.02 Da. Fixed modification was set to carbamidomethylation of cysteine, and variable modification was set to oxidation of methionine. Two missed cleavages by trypsin were allowed.

RESULTS

HCoV-229E predominantly uses endocytosis for cellular entry

In order to elucidate the molecular mechanism of coronavirus entry into cells, we first made an attempt to purify coronavirus particles. This was done by 10–50% sucrose density gradient ultracentrifugation method (Fig. 1A). Briefly, we infected human hepatocellular carcinoma-derived Huh7 cells with HCoV-229E, and the supernatant was collected after 1 week. The viral fraction was identified by SDS-PAGE followed by Coomassie Brilliant Blue (CBB) staining of samples fractionated by sucrose density gradient (Fig. 1B). The fractions numbered 9 to 11, in which nucleoproteins were found to be the most abundant in the viral particles, were collected and concentrated to produce purified viral samples. TCID50 of the purified virus was measured in Huh7 cells, and a titer of 10⁸ /mL was obtained.

As a next step, we confirmed cellular uptake and infection of the purified virus particles. For this, Huh7 cells were infected at MOI =1, cells were collected successively, and newly synthesized viral nucleoprotein was confirmed by Western blot (Fig. 1C). To confirm endocytic uptake of HCoV-229E and to quantify viral infection efficiency, we treated the cells with the viral particles in the presence or absence of an endosomal inhibitor Bafilomycin A1. Viral infection was significantly suppressed in the Bafilomycin A1 treated samples as shown by quantitative RT-PCR viral infection efficiency assay in Fig. 1D. Similar results were obtained when the efficiency of viral infection of Bafilomycin-treated cells was examined by immunofluorescent analysis (Supplemental Fig.1A and B). These results clearly suggest that HCoV-229E enters Huh7 cells by endosome-dependent endocytosis. Our data are consistent with the phenomenon of HCoV-229E uptake in clathrin-mediated endocytosis, as recently reported by Andreu et al.¹⁵

To further confirm the behaviour of the viral particles in cells, immunostaining was used to detect coronavirus nucleoproteins and early endosome markers Rab5A and/or EEA1 at half an hour or two hours post infection at MOI=5 or 10. As shown in Fig. 1E, both nucleoproteins and Rab5A and/or EEA1 co-localised in the cytoplasm confirming that purified HCoV-229E enters cells via endosomes.

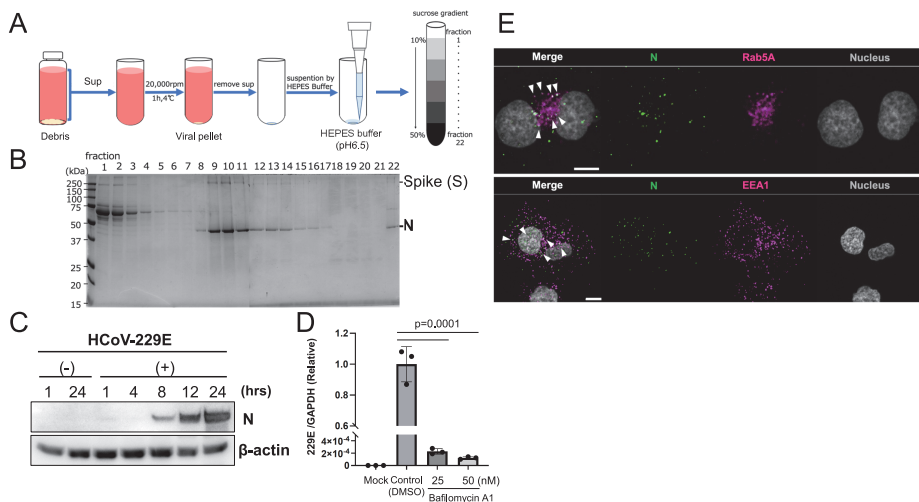


Fig. 1 High-titer coronavirus purification

Fig. 1A: Schematics of virus purification steps. HCoV-229E and/or HCoV-OC43 were infected in Huh7 cells at 35 °C for more than one week. Supernatant of cell culture was harvested by low-speed centrifugation and followed to ultracentrifugation. Viral pellets were suspended in HEPES buffer, and the viral fraction was fractionated by sucrose density gradient ultracentrifugation.

Fig. 1B: SDS-PAGE and CBB staining of viral fractions. Nucleoprotein was highly detected in fractions no. 9–11, and these fractions were pooled and concentrated as final purified virus fraction.

Fig. 1C: Purified viruses infect cultured cells. The titer of purified viral samples was determined by TCID₅₀, and the expression of nucleoprotein (N) when infected with Huh7 cells at MOI=1 was confirmed by Western blot.

Fig. 1D: HCoV-229E is taken up into cells by endocytosis. Results of RT-qPCR quantification of viral infection after 24 hours. Viral uptake measured by RT-qPCR was completely inhibited by Bafilomycin A1 treatment. Unpaired student's t-test; P=0.0001.

Fig. 1E: Subcellular distribution of nucleoproteins 0.5 or 2 hours post infection at MOI=5 or 10. Viral nucleoproteins were stained with anti-Rab5A and/or EEA1 antibodies (shown in magenta). Co-localisation signals were shown in the arrowhead. The green signal shows nucleoproteins. Scale bar: 10 μm.

SDS-PAGE: sodium dodecyl sulfate polyacrylamide gel electrophoresis

CBB: coomassie brilliant blue

TCID₅₀: tissue culture infectious dose 50

MOI: multiplicity of infection

RT-qPCR: real-time quantitative polymerase chain reaction

Ubiquitin content within the viral particles

IAVs are taken up by host cells by endocytosis, followed by membrane fusion in late endosomes. Previous reports indicate that the unanchored ubiquitin chains contained within its own particles are used to facilitate the uncoating step.^{6,7} To clarify whether a similar mechanism promotes the uncoating from endosomes in coronaviruses, we examined the presence of ubiquitin molecules in purified viral particles by Western blot. As a control, we used purified IAV to compare with HCoV-OC43, and the purity of the used viruses was checked under TEM. Surface glycoproteins and Spike proteins were clearly visible on the outside of both influenza and coronaviruses (Fig. 2A). Next, to investigate the nature of the ubiquitin chains in the various viral particles, ubiquitin signals were detected by various antibodies against ubiquitin chains. Anti-ubiquitin (FK2) mouse monoclonal antibody recognizes endogenous levels of total ubiquitin protein. This antibody detects conjugates but not free ubiquitin. Anti-ubiquitin antibody (P4D1)

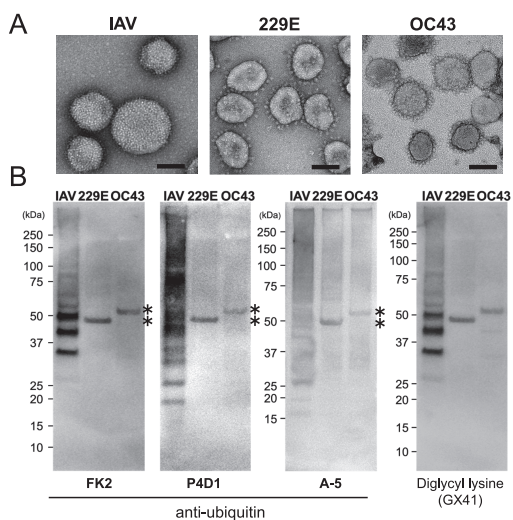


Fig. 2 Unanchored ubiquitin is not detected within purified seasonal coronavirus particles

Fig. 2A: TEM images of various viruses. Left, influenza A virus (IAV); center, HCoV-229E; right, HCoV-OC43. Scale bar shows 100 nm.

Fig. 2B: Detection of ubiquitin chains within viral extracts, 16.8 μ g, 12.7 μ g, and 27.8 μ g of IAV, HCoV-229E, and HCoV-OC43 viral extract were loaded, respectively. Ubiquitin signals were detected with various anti-ubiquitin and anti-diglycyl lysine antibodies. Asterisks indicate non-specific signals.

TEM: transmission electron microscopy

HCoV: human coronavirus

recognizes whole ubiquitin molecules (Monoclonal antibody is produced by immunizing animals with 1–76 full length bovine ubiquitin). Anti-ubiquitin antibody (A-5) raised against amino acids 1–76 representing the full-length ubiquitin of human origin. The results showed that a ladder of unanchored ubiquitin chains could be detected in IAV, whereas both HCoV-229E and HCoV-OC43 had no such detectable ladder signals (Fig. 2B). A signal around 50 kDa detected by the anti-ubiquitin antibodies in HCoV-229E and HCoV-OC43 was excised from the gel and treated with trypsin (or Asp-N) to identify the ubiquitin molecule by mass spectrometry analysis, but no ubiquitin-derived peptide could be detected (data not shown). However, the fact that deubiquitinated peptides have been detected with anti-diglycyl lysine antibodies suggests that deubiquitinated proteins around 50 kDa may be present within the viral particles. (Fig. 2B, right panel). These results suggest that, unlike IAV, unanchored ubiquitin chains may not be used in the uncoating reaction of coronaviruses from endosomes.

In vitro uncoating reveals RNA genome condensation during endosomal maturation

Next, we focused on the changes that might occur inside the viral particle when its interior is acidified by endosome maturation. *In vitro* uncoating is a method developed by Stauffer et al to detect changes in the state of the internal viral genome by removing the membrane component of the virus.^{13,14,16} The status of the internal viral genome was observed by removing the viral membrane by an *in vitro* uncoating method to see whether acidification within the endosome affected the structure of the nucleocapsid inside the virus. Briefly, viral particles are added to a buffer solution with a two-layer glycerol gradient followed by ultracentrifugation. The lower layer of glycerol buffer contains 1% NP-40, which makes it possible to remove the viral membrane to observe its internal genomic structure (Fig. 3A). The pH in endosomes can also be mimicked

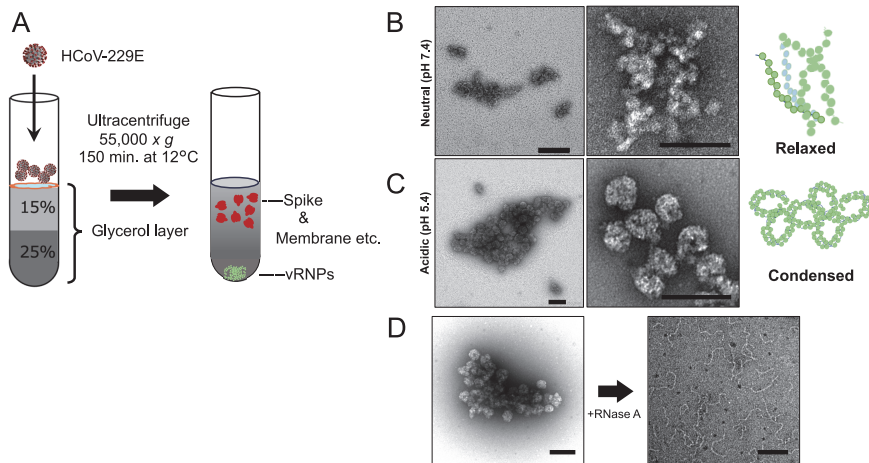


Fig. 3 In vitro uncoating reveals nucleocapsid condensation in the endosome

Fig. 3A: Schematic diagram of in vitro uncoating. Purified coronaviruses were placed on top of a buffer containing two layers of 15% and 25% glycerol buffer, and performed ultracentrifugation. The lower buffer containing 25% glycerol and 1% NP-40 was ultracentrifuged at pH 7.4 and pH 5.4, respectively. The vRNPs are fractionated into pellet fractions, while the spike and membrane fractions are fractionated into upper layers.

Fig. 3B, C: TEM image of the pellet fraction after ultracentrifugation. Loosely clustered vRNPs were observed under neutral conditions (pH 7.4; B), whereas under acidic conditions (pH 5.4; C), which mimicked endosomal conditions, vRNPs of the size derived from a single virus particle were observed to aggregate individually. Scale bar: 200 nm.

Fig. 3D: Clumps of vRNPs are dissociated into RNA strands by RNase A treatment. TEM image of pellet fractions obtained under pH 5.4 conditions after digestion with RNase A treatment at 37 °C for 30 minutes. Scale bar: 200 nm.

vRNP: viral ribonucleoprotein

TEM: transmission electron microscopy

by changing the pH of the lower buffer solution. After ultracentrifugation, the pellet fractions were suspended and observed by TEM. The results showed that the nucleocapsids obtained under neutral conditions were loosely spread in shape, whereas the nucleocapsids obtained under acidic conditions formed a particle-by-particle condensate structure (Fig. 3B and C). To ensure that the condensate structures are nucleocapsids containing RNA, pellet samples are digested with RNase A and observed by TEM. As a result, the condensate structure disappeared after RNase A treatment, and string-like fragmented nucleocapsids were detected (Fig. 3D). In other words, the condensates obtained by in vitro uncoating were found to be aggregates of nucleocapsids under acidic conditions.

DISCUSSION

Compared to IAV, ubiquitin chains in the viral particles of HCoV-229E and HCoV-OC43 amplified and purified from Huh7 cells were almost in an undetectable level. As IAV has unanchored ubiquitin chains in its particles, vRNPs are released into the cytoplasm after M1 shell disassembly by the unanchored ubiquitin-binding and Dynein-binding activities of the host deacetylase HDAC6.^{7,8} Therefore, it can be inferred that the uncoating in coronaviruses does not utilise the HDAC6 pathway with unanchored ubiquitin chains. This observation also suggests that there is

a molecular mechanism by which ubiquitin is actively excluded during viral RNA packaging and viral particle formation at the ER-Golgi intermediate compartment, so-called ERGIC. Regulation of coronavirus proteins by ubiquitination and/or SUMOylation has been reported.¹⁷⁻²¹ For example, the nucleoprotein of SARS-CoV-2 was reported to be involved in the interaction with the RNA genome through K29-linked ubiquitination of the nucleoprotein by host TRIM6. This phenomenon is thought to be conserved only in SARS-CoV and not in seasonal coronaviruses.¹⁷ Others have reported that ubiquitination of K15 of SARS-CoV-2 M protein promotes the formation of viral particles.¹⁸ This report shows that the M protein is ubiquitinated in HEK293T cells, but it has not been confirmed whether the viral particles released from the cells contain ubiquitin. Also, the K15 residue on the M protein is not conserved in other coronaviruses and may involve a specific regulatory mechanism for SARS-CoV-2. It is also possible that the ubiquitination sites suggested in this study are located outside the viral membrane and that viral particles are formed in the ERGIC and deubiquitinated before they are released outside the cell. Other studies have shown that the host deubiquitinating enzyme USP22 suppresses degradation of SARS-CoV-2 nucleoprotein by inhibiting ubiquitination on K375, contributing to virus production.¹⁹ TRIM21 controls degradation of SARS-CoV-2 nucleoprotein by ubiquitination of K375 and regulation of multimerisation and viral particle formation by SUMOylation of nucleoprotein K62 of SARS-CoV have also been reported,^{20,21} the details of which are controversial. On the other hand, seasonal coronaviruses have only limited ubiquitin in their viral particles, which may facilitate nucleocapsid uncoating by serving as a substrate for ubiquitination during viral infection. Viral condensates formed by endosomal acidification are thought to prevent long single-stranded RNA genomes from being sensed by host innate immune responses (Fig. 4A). In general, host immune response is activated by viral double-stranded RNAs (dsRNAs). The immune response to viral infection often begins when viral dsRNA is detected by dsRNA-binding proteins in the host. These sensors include RIG-I-like receptors (RLRs), protein kinase R (PKR), oligoadenylate synthases (OASes), Toll-like receptors (TLRs) and NOD-, LRR- and pyrin domain-containing 1 (NLRP1).²² During endocytic entry of coronavirus, viral genomes are uncoated from the endosome. Just after uncoating, the viral genome of coronavirus should be single-stranded RNA. Therefore, these RNA genomes might not be detected by host immune factors. However, it is possible that coronavirus RNAs with a 5' cap structure and short stem loop in 5' and 3' untranslated region (UTR) may be recognized by PKR.^{23,24} To avoid recognition by PKR, the viral genome might form an aggregate during uncoating. The RNase-resistant phase separation may be formed by viral aggregates, which may improve the efficiency of uncoating and prevent attack by RNases in the cell. Since in vitro experiments have shown that viral genome aggregates are cleaved to some extent by RNase A treatment, we would like to limit ourselves to the expression that it is conceivable that they may escape attack from RNase by phase-separating at the physiological condition within the cell. It is possible that nucleocapsid condensate formation due to endosomal acidification may increase the efficiency of the uncoating reaction from the endosome (Fig. 4B).

Recently, genome-wide small interfering RNA (siRNA) screens in infectious bronchitis virus have reported the involvement of the host factor VCP/p97 in uncoating from endosomes, and the inhibition of VCP/p97 has been observed to result in the accumulation of virus in early endosomes. The defective VCP/p97 inhibited the degradation of nucleocapsid proteins.²⁵ Nucleocapsid degradation has been suggested to involve the proteasome system, but the details of its regulation via ubiquitin are not clear. VCP/p97 has been reported to be involved in ubiquitin metabolism, and its involvement in endosomal maturation and recycling endosomes has also been suggested.^{26,27} The dengue virus, which causes dengue fever, and the Zika virus, which is transmitted by ticks and mosquitoes, both belong to the *Flaviviridae* family, which has a positive single-stranded RNA genome like a coronavirus. VCP/p97 has been reported to be involved in the

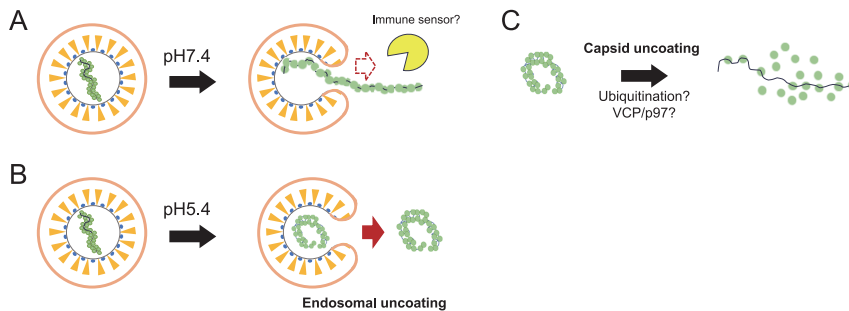


Fig. 4 The role of acidification for coronavirus uncoating

Fig. 4A: When membranes fuse under neutral conditions, loose RNA genomes are more likely to be recognised by host innate immune response factors if they are uncoated, affecting infection efficiency.

Fig. 4B: Nucleocapsids exposed to acidification as endosomes mature may form aggregates, thereby increasing their uncoating efficiency from endosomes and escaping from host immune surveillance factors.

Fig. 4C: vRNPs that are uncoated as nucleocapsid condensates might be subsequently ubiquitinated, and VCP/p97 may promote capsid uncoating to initiate translation.

vRNP: viral ribonucleoprotein

VCP: valosin-containing protein

uncoating of these viral genomes.²⁸ It has also been suggested that ubiquitination modification of the viral genome released into the cytoplasm following fusion of the virus with the endosomal membrane may act as a nucleocapsid uncoating factor.²⁹ In fact, VCP inhibitor NMS-873 blocked HCoV-229E infection in Huh7 cells (Supplemental Fig. 1C and D).³⁰ Given these considerations, we would like to propose a new hypothesis that ubiquitin-free nucleocapsid condensates formed by liquid-liquid phase separation are ubiquitinated by ubiquitinating enzymes immediately after uncoating, thus becoming a substrate for VCP/p97 and capsid uncoating is promoted (Fig. 4C). VCP/p97 is thought to function together with HDAC6 in the regulation of protein aggregates and stress granules, therefore further molecular mechanisms of HCoV uncoating step are expected to be elucidated in the future and led to new drug development.

AUTHOR CONTRIBUTIONS

MU performed all experiments. KY performed IF analysis. YS prepared cell lines and HCoV strains, produced anti-N antibodies. YM designed all experiments and wrote the manuscript. HK oversaw this project, and all authors contributed to finalize the manuscript.

COMPETING INTERESTS

The authors declare no competing interests.

FUNDING/SUPPORT

This work was financially supported by the COVID-19 fund of Sumitomo Mitsui Trust Bank and JST SPRING, Grant Number JPMJSP2125. This work was also supported by JST PRESTO (Grant Number JPMJPR19H5) to YS, JST FOREST Program (Grant Number JPMJFR206B) to

YM, JSPS KAKENHI (Grant-in-Aid for Scientific Research (C)) Grant Number JP20K07513 & JP23K06572 for YM, and AMED-CREST (Grant Number JP25gm1610001) for HK.

ADDITIONAL CONTRIBUTIONS

The authors wish to acknowledge Division for Medical Research Engineering, Nagoya University Graduate School of Medicine, for technical support of electron microscopy, Dr Koji Itakura, and mass spectrometry analysis, Dr Kentaro Taki. We also thank Dr Longlong Wang (ETH Zurich) and Dr Anand Manoharan for critically reading our manuscript, all members of the Virology lab for valuable comments, Ms Tomoko Kunogi for technical assistance, and Dr Jiro Usukura (Nagoya University) for technical suggestions for the electron microscope.

ACKNOWLEDGEMENT

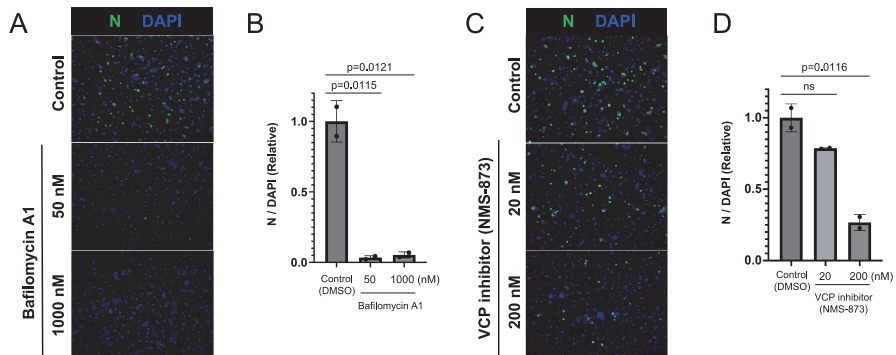
MU would like to take this opportunity to thank Interdisciplinary Frontier Next-Generation Researcher Program of the Tokai Higher Education and Research System.

REFERENCES

- 1 V'kovski P, Kratzel A, Steiner S, Stalder H, Thiel V. Coronavirus biology and replication: implications for SARS-CoV-2. *Nat Rev Microbiol.* 2021;19(3):155–170. doi:10.1038/s41579-020-00468-6
- 2 Blau DM, Holmes KV. Human coronavirus HCoV-229E enters susceptible cells via the endocytic pathway. *Adv Exp Med Biol.* 2001;494:193–198. doi:10.1007/978-1-4615-1325-4_31
- 3 Tsai YX, Chien YC, Hsu MF, Khoo KH, Hsu SD. Molecular basis of host recognition of human coronavirus 229E. *Nat Commun.* 2025;16(1):2045. doi:10.1038/s41467-025-57359-8
- 4 Shirato K, Kanou K, Kawase M, Matsuyama S. Clinical Isolates of Human Coronavirus 229E Bypass the Endosome for Cell Entry. *J Virol.* 2016;91(1):e01387-16. doi:10.1128/JVI.01387-16
- 5 Helenius A. Virus Entry: Looking Back and Moving Forward. *J Mol Biol.* 2018;430(13):1853–1862. doi:10.1016/j.jmb.2018.03.034
- 6 Yamauchi Y. Influenza A virus uncoating. *Adv Virus Res.* 2020;106:1–38. doi:10.1016/bs.aivir.2020.01.001
- 7 Banerjee I, Miyake Y, Nobs SP, et al. Influenza A virus uses the aggresome processing machinery for host cell entry. *Science.* 2014;346(6208):473–477. doi:10.1126/science.1257037
- 8 Wang L, Moreira EA, Kempf G, et al. Disrupting the HDAC6-ubiquitin interaction impairs infection by influenza and Zika virus and cellular stress pathways. *Cell Rep.* 2022;39(4):110736. doi:10.1016/j.celrep.2022.110736
- 9 Miyake Y, Keusch JJ, Decamps L, et al. Influenza virus uses transportin 1 for vRNP debundling during cell entry. *Nat Microbiol.* 2019;4(4):578–586. doi:10.1038/s41564-018-0332-2
- 10 Cros JF, Palese P. Trafficking of viral genomic RNA into and out of the nucleus: influenza, Thogoto and Borna disease viruses. *Virus Res.* 2003;95(1-2):3–12. doi:10.1016/s0168-1702(03)00159-x
- 11 Iserman C, Roden CA, Boerneke MA, et al. Genomic RNA Elements Drive Phase Separation of the SARS-CoV-2 Nucleocapsid. *Mol Cell.* 2020;80(6):1078–1091.e6. doi:10.1016/j.molcel.2020.11.041
- 12 Carlson CR, Asfaha JB, Ghent CM, et al. Phosphoregulation of Phase Separation by the SARS-CoV-2 N Protein Suggests a Biophysical Basis for its Dual Functions. *Mol Cell.* 2020;80(6):1092–1103.e4. doi:10.1016/j.molcel.2020.11.025
- 13 Stauffer S, Nebioglu F, Helenius A. In vitro Disassembly of Influenza A Virus Capsids by Gradient Centrifugation. *J Vis Exp.* 2016;109:e53909. doi:10.3791/53909
- 14 Miyake Y, Hara Y, Umeda M, Banerjee I. Influenza A Virus: Cellular Entry. *Subcell Biochem.* 2023;106:387–401. doi:10.1007/978-3-031-40086-5_14
- 15 Andreu S, Ripa I, López-Guerrero JA, Bello-Morales R. Human Coronavirus 229E Uses Clathrin-Mediated Endocytosis as a Route of Entry in Huh-7 Cells. *Biomolecules.* 2024;14(10):1232. doi:10.3390/biom14101232
- 16 Stauffer S, Feng Y, Nebioglu F, Heilig R, Picotti P, Helenius A. Stepwise priming by acidic pH and a high

- K+ concentration is required for efficient uncoating of influenza A virus cores after penetration. *J Virol.* 2014;88(22):13029–13046. doi:10.1128/JVI.01430-14
- 17 Zhou J, Zhou Y, Wei XF, et al. TRIM6 facilitates SARS-CoV-2 proliferation by catalyzing the K29-typed ubiquitination of NP to enhance the ability to bind viral genomes. *J Med Virol.* 2024;96(3):e29531. doi:10.1002/jmv.29531
 - 18 Yuan Z, Hu B, Xiao HR, et al. The E3 Ubiquitin Ligase RNF5 Facilitates SARS-CoV-2 Membrane Protein-Mediated Virion Release. *mBio.* 2021;13(1):e0316821. doi:10.1128/mbio.03168-21
 - 19 Xiao X, Li S, Zheng Z, et al. Targeting USP22 to promote K63-linked ubiquitination and degradation of SARS-CoV-2 nucleocapsid protein. *J Virol.* 2025;99(5):e0223424. doi:10.1128/jvi.02234-24
 - 20 Mao S, Cai X, Niu S, et al. TRIM21 promotes ubiquitination of SARS-CoV-2 nucleocapsid protein to regulate innate immunity. *J Med Virol.* 2023;95(4):e28719. doi:10.1002/jmv.28719
 - 21 Li FQ, Xiao H, Tam JP, Liu DX. Sumoylation of the nucleocapsid protein of severe acute respiratory syndrome coronavirus. *FEBS Lett.* 2005;579(11):2387–2396. doi:10.1016/j.febslet.2005.03.039
 - 22 Chen YG, Hur S. Cellular origins of dsRNA, their recognition and consequences. *Nat Rev Mol Cell Biol.* 2022;23(4):286–301. doi:10.1038/s41580-021-00430-1
 - 23 Malone B, Urakova N, Snijder EJ, Campbell EA. Structures and functions of coronavirus replication-transcription complexes and their relevance for SARS-CoV-2 drug design. *Nat Rev Mol Cell Biol.* 2022;23(1):21–39. doi:10.1038/s41580-021-00432-z
 - 24 Nallagatla SR, Hwang J, Toroney R, Zheng X, Cameron CE, Bevilacqua PC. 5'-triphosphate-dependent activation of PKR by RNAs with short stem-loops. *Science.* 2007;318(5855):1455–1458. doi:10.1126/science.1147347
 - 25 Wong HH, Kumar P, Tay FP, Moreau D, Liu DX, Bard F. Genome-Wide Screen Reveals Valosin-Containing Protein Requirement for Coronavirus Exit from Endosomes. *J Virol.* 2015;89(21):11116–11128. doi:10.1128/JVI.01360-15
 - 26 Boyault C, Gilquin B, Zhang Y, et al. HDAC6-p97/VCP controlled polyubiquitin chain turnover. *EMBO J.* 2006;25(14):3357–3366. doi:10.1038/sj.emboj.7601210
 - 27 Kawan M, Körner M, Schlosser A, Buchberger A. p97/VCP Promotes the Recycling of Endocytic Cargo. *Mol Biol Cell.* 2023;34(13):ar126. doi:10.1091/mbc.E23-06-0237
 - 28 Ramanathan HN, Zhang S, Douam F, et al. A Sensitive Yellow Fever Virus Entry Reporter Identifies Valosin-Containing Protein (VCP/p97) as an Essential Host Factor for Flavivirus Uncoating. *mBio.* 2020;11(2):e00467–20. doi:10.1128/mBio.00467-20
 - 29 Byk LA, Iglesias NG, De Maio FA, Gebhard LG, Rossi M, Gamarnik AV. Dengue Virus Genome Uncoating Requires Ubiquitination. *mBio.* 2016;7(3):e00804–16. doi:10.1128/mBio.00804-16
 - 30 Cheng KW, Li S, Wang F, Ruiz-Lopez NM, Hauerbi N, Chou TF. Impacts of p97 on Proteome Changes in Human Cells during Coronaviral Replication. *Cells.* 2021;10(11):2953. doi:10.3390/cells10112953

SUPPLEMENTARY INFORMATION



Suppl Fig. 1 Bafilomycin A1 and the VCP inhibitor block coronavirus infection

Suppl Fig. 1A: Immunofluorescent images after HCoV-229E infection in Huh7 cells. Cells were treated with or without endosome inhibitor Bafilomycin A1. Infected cells were detected by anti-nucleoprotein (N) antibody (shown in green). Nuclei were counterstained with DAPI (shown in blue).

Suppl Fig. 1B: Quantification of nucleoprotein-positive (infected) cells from panel A by high-throughput imaging BZ-X800 (Keyence). The number of infected cells in the untreated control is set as 1. Statistical significances were confirmed by an unpaired Student's t-test.

Suppl Fig. 1C: Immunostaining experiment as in A with or without VCP inhibitor (NMS-873). Nucleoprotein represented in green, and the nucleus was counterstained with DAPI in Blue.

Suppl Fig. 1D: Quantification of nucleoprotein-positive (infected) cells from panel C by high-throughput imaging BZ-X800 (Keyence). The number of infected cells in the untreated control is set as 1. Statistical significances were confirmed by an unpaired Student's t-test.

HCoV: human coronavirus

DAPI: 4',6-diamidino-2-phenylindole

VCP: valosin-containing protein

ns: not significant